Structural and theoretical studies of 4,4'-[1,4-phenylene-bis-(azanediyl)]dipent-3-en-2-one: evidence of a π-delocalized keto-enamine

O. T. Benjelloun,[a] M. Akkurt,[b] S. Ö. Yıldırım,[b] M. Daoudi,[a] T. Ben Hadda,[c*] A. Boukir,[a] O. Büyükgüngör,[d] and A. F. Jalbout[e*]

[a]Laboratorie de Chimie Organique, Faculté des Sciences, Dhar Mehraz, 30000 Fès, Morocco
[b]Department of Physics, Faculty of Arts and Sciences, Erciyes University, 38039 Kayseri, Turkey
[c]Laboratoire de chimie des Matériaux, Faculté des Sciences, 60000 Oujda, Morocco
[d]Department of Physics, Faculty of Arts and Sciences, Ondokuz Mayıs University, 55139 Samsun, Turkey
[e]Instituto de Quimica, Universidad Nacional Autonoma de Mexico, Mexico D.F.
E-mail: tbenhadda@yahoo.fr, ajalbout@email.arizona.edu

Abstract

In this work we present the synthesis of 4,4'-[1,4-phenylene-bis(azanediyl)]dipent-3-en-2-one. Evidence is proposed for the presence of various tautomers of this molecule which are complemented with theoretical density functional theory (DFT)-B3LYP/6-31G* calculations to characterize the potential energy surface of these species. The experimentally observed **3b** isomer crystallizes as an orthorhombic *Pbcn* structure; a = 10.8412(10) Å, *b* = 8.9205(7)Å, c = 14.9949(13)Å, V = 1450.1(2) Å^3, Z = 4 with a final *R* value is 0.038. From our X-Ray crystallographic analysis an intramolecular hydrogen N-H···O interaction is observed.

Keywords: Bis-N,O-ligand, tautomeric forms, geometrical parameters, DFT methods

Introduction

Metallo-organic complexes containing conjugated nitrogen ligands represent an important class of nonlinear optical chromophores.[1] Efficient systems involving organometallic and coordination compounds with donor-acceptor bipyridyl,[2] bipyridyl ligand bearing azo and imino-linked dyes,[3] enamines,[4] or Schiff-bases ligands have the focus of other recent works.[5] The direct impact of dipolar effects in drug design of functionalised bis-armed quinoxaline has been suitability demonstrated [6a] as well as that with 3-nitrozo-imidaz[1,2-*a*]pyridines.[6b] Additionally, the synthesis of square-pyramidal $[Co_2Cl_2L_2]Cl_2$ (HL = *m*-phenylenediiminobis(acetylacetone) (I), *p*-phenylenediiminobis(acetylacetone) (II), *p*-diphenyldiiminobis(acetylacetone) (III)) has been

described by others[6c]. The corresponding ESR measurements show intra-dimer zero splitting and tetradentate coordination through both O and N atoms as in the present investigation.

In corroboration with our research involving DNA intercalators, we have developed an interest in the elaboration of highly conjugated bidentate heterocyclic ligands. The 4,4'-[1,4-phenylene-bis(azanediyl)]dipent-3-en-2-one **3**, reported in this work can be described as symmetric tautomers in the bis-(keto-imine) form (**3a**). Other forms that are observed are the bis-(keto-en-amine) form (**3b**), the bis-(enol-imine) form (**3c**), the dissymmetric tautomers in the (enol-imine/keto-en-amine) form (**3d**), possibly even the (enol-imine/keto-imine) form (**3e**) and finally the (keto-en-amine/keto-imine) geometrical structure (**3f**). The tautomeric structure (**3c**) is of particular interest since it presents an extended conjugated pathway with a potentially bis(bidentate) N,O-ligand. The basic synthesis of the bis-bidentate N,O-ligand 4,4'-[1,4-phenylene-bis (azanediyl)]dipent-3-en-2-one **3** has been depicted in Scheme 1.

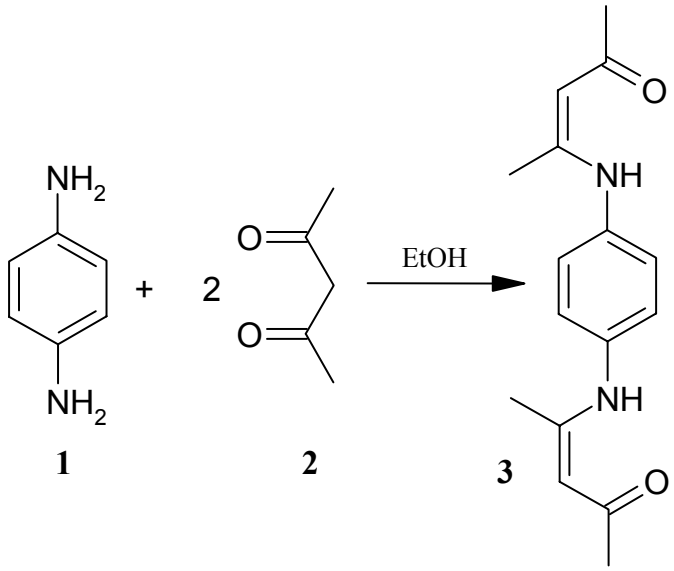

Scheme 1. Synthesis of the 4,4'-[1,4-phenylenebis (azanediyl)]dipent-3-en-2-one (**3**) described in this work.

Results and Discussion

It is difficult to elucidate the correct tautomeric from the IR spectra of compound **3**. The hydrogen-bonded N-H bands are extremely weak and broad, spanning from about 3700 to 2700 cm^{-1} with the center somewhere between 3400 and 2900 cm^{-1}, by which this region includes the C-H vibrations as well. There is only a difference of 1% transmittance between the peak center and the baseline which makes this a difficult task indeed. The C-C ring stretching mode is clearly shown as a strong band at about 1562 cm^{-1} however, the carbonyl stretch is nearly masked as a

weak band at 1608 cm^{-1}. This latter mode has been assigned in the position isomer compound labeled as 4,4'-[1,3-phenylenebis (azanediyl)]dipent-3-en-2-one previously described.[5d]

Theoretical methods

Theoretical computations were performed to complement the experiments being described in the present experimental measurements. All calculations in this work where carried out with the AM1 level of theory as well as the Density Functional Theory (DFT)-B3LYP/6-31G* level of theory using the GAUSSIAN03 suite of programs.[7] NMR shifts were computed using the GIAO method, and referenced relative to TMS for consistancy. Further information about these methods is available elsewhere.[8] Previously reported,[9] carbon shifts (in TMS) at the B3LYP/6-311+G(2d,2p) level are 182.4572 ppm, and the hydrogen shift (in TMS) are 31.6297 ppm.

Figure 1 (based on the representative structures shown in Scheme 2) depict the optimized structures computed at the B3LYP/6-31G* level of theory. The theoretical vibrational spectrum are shown in Figure 2. In the structural representation, all bond lengths are in angstroms (Å) and bond angles are in degrees (°). For the theoretical vibrational spectra, the frequencies are in cm^{-1}, and the IR intensities in KM/mol (broadened by the Doppler method).

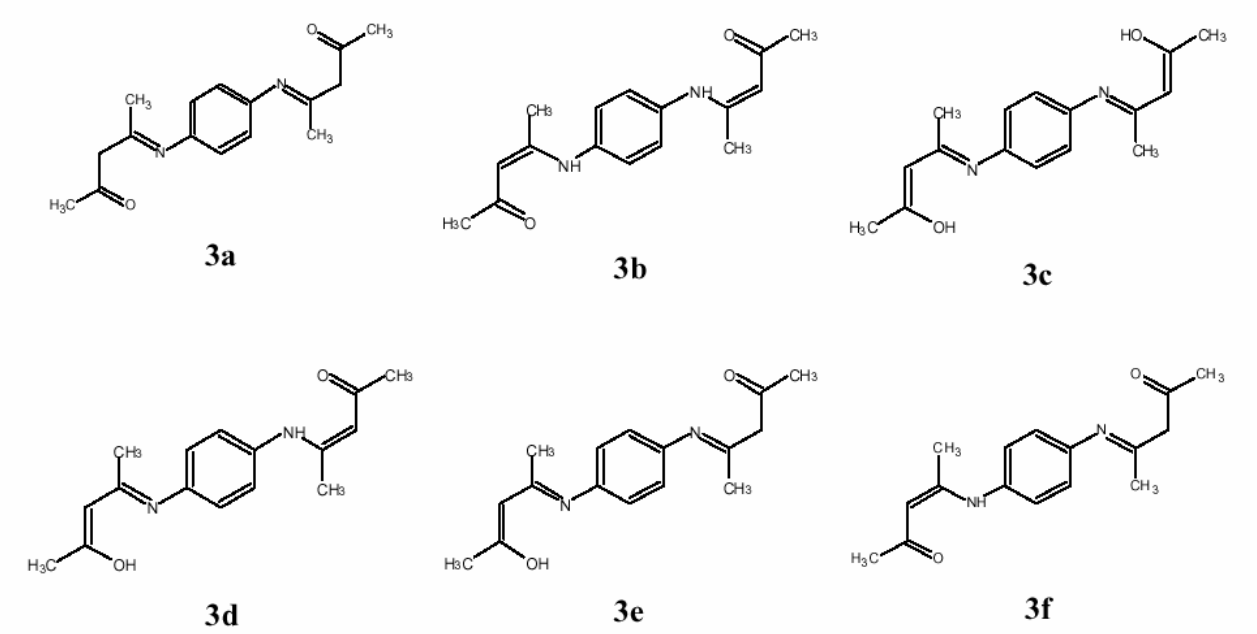

Scheme 2. Different tautomeric forms of *para*-phenylenediamine derivative **3**.

Generally speaking, the AM1 and B3LYP/6-31G* geometrical and thermodynamic results were similar with an RMSD value of 0.2724, 1.1504, 0.4678, 0.52554, 0.29085, 0.27761 for **3a-3f** geometrical parameters, respectively. The largest difference in the structures was calculated for **3b** but it is still minimal in comparison. This difference might be accounted for the complex nature of this species with respect to the other structures examined. The RMSD used is the

relative differences in geometrical parameters for each structure computed at the AM1 and DFT level of theory. Figure 1 depicts various selected geometrical parameters for the structures however Table 4 displays both experimental and theoretical B3LYP/6-31G* data for the observed **3b** isomer. As we can see the relative deviation is quite low and it serves as an example of the efficacy of the DFT methods in evaluating the physical properties of organic structures.

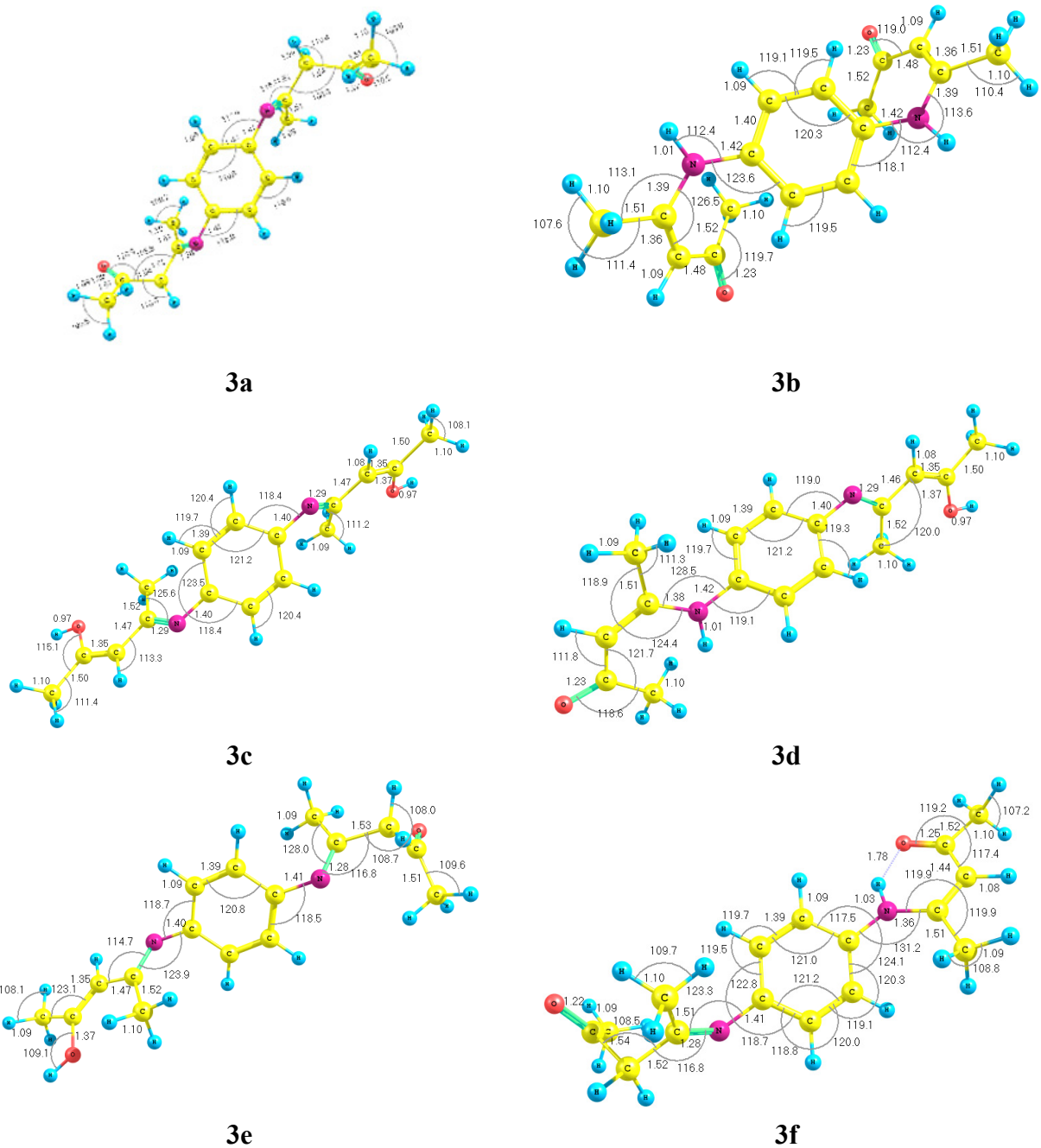

Figure 1. B3LYP/6-31G* structures are shown for the six different tautomeric forms of *para*-phenylenediamine derivatives. All bond lengths are shown in angstroms (Å) and bond angles are shown in degrees (°)

Table 1 presents the relative energies for the structures in kcal/mol. The table shows that the lowest energy structure is **3f** (which is given a relative energy value of 0.0). As we can see the AM1 and B3LYP results are substantially different. It is known,[9] that AM1 and B3LYP give similar geometries, but rather different energies, as is apparent from the table. This is relevant since both methods are derived from semi-empiracle models, however, it is logical that the DFT method has electron correlation which exceeds AM1 in energetic computations. Therefore, it can be expected that differences should exist which are observed, however the general trends remain consistantly similar which provides an an order of stability are **3f**>**3a**>**3e**>**3b**>**3d**>**3c**. The differences in energy can be reasoned by an observation of the structures.

Table 1. Total energies (hartrees/particle) and relative energies (kcal/mol) relative to the lowest energy structure (**3f**). 0 K is the sum of zero-point and electronic energies

	AM1	AM1 (0 K)	B3LYP/ 6-31G*	B3LYP/ 6-31G* (0 K)
3a	-0.0423211	0.295334	-881.6830603	-881.3517540
3b	-0.0258598	0.313005	-881.6620746	-881.3291020
3c	-0.0132183	0.324486	-881.6421844	-881.3103650
3d	-0.0232351	0.315578	-881.6579686	-881.3253650
3e	-0.0283841	0.309450	-881.6635313	-881.3318630
3f	-0.0473310	0.291417	-881.6964744	-881.3638790
ΔE^{3a}	3.144	2.458	8.417	7.608
ΔE^{3b}	13.473	13.546	21.586	21.823
ΔE^{3c}	21.406	20.751	34.067	33.580
ΔE^{3d}	15.120	15.161	24.162	24.168
ΔE^{3e}	11.889	11.316	20.672	20.090
ΔE^{3f}	0.0	0.0	0.0	0.0

The **3f** molecule has internal hydrogen bonding that stabilizes the structure, as has been seen for the other structures which also posses internal hydrogen bond stabilization. The compounds without–NH groups are also stabilized (i.e. **3a**, **3e**) in comparison to those that do (**3b**, **3d**). The final structure **3c** lacks stability due to the orientation of internal amino groups. We have attempted to locate forms of the structures **3c**, **3d**, **3e** that form N—OH hydrogen bonds but these were only partially stable. The bond order between these was around 0.005 which is less than that of 0.10 for a typical hydrogen bond. While it is a viable mechanism for molecular stabilization it certainly is not the only factor but should be considered. The structures presented are the lowest energy isomers that we were able to calculate along the potential energy surface.

Along a similar note, in **3b** there are two hydrogen bonds between NH and CO that form and in **3c** between N and OH. Of course in **3d** the N—OH and NH---CO hydrogen bonds also tend to stabilize the molecule but as the energies suggest the stability that arises from the NH---CO hydrogen bonds are ideal. The relative stabilities of **3b** and **3d** are higher than that observed for

3c due to the presence of NH---CO interactions. This is an important concept, since the NH---CO bond order is around 0.12 that is considered to be strong and lead to internal molecular stabilization.

Figure 2 displays the spectra for the tautomers. Therefore, it would appear that **3c**, **3e** share similar peaks due to the similar structure, and **3a**, **3e** as well as **3b**, **3d** also share similar peaks, again owing to their similar geometries. Experimentally we believe **3a** and **3f** will be the highest product of observed species. As we can see from the figures it is clear that peaks at around 1560 cm^{-1} which correspond to the C=O stretches can be observed in the structures as well as those for the C=N stretches at around 1510 cm^{-1}.

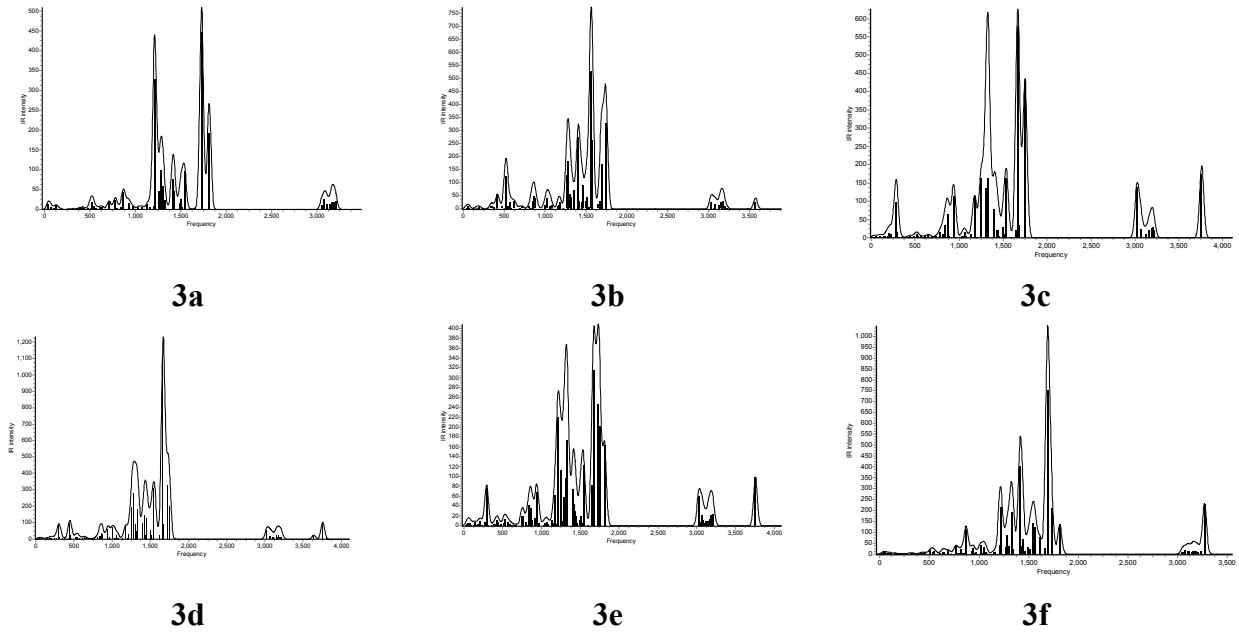

Figure 2. B3LYP/6-31G* theoretical IR vibrational spectra, where the frequencies are shown in cm^{-1}, and intensities in KM/mol. Peaks are broadened by the Doppler broadening method.

For the **3b** structure it appears that they are shifted towards the experimental value of 1562 cm^{-1} for the C=O shifts. In the **3f** case we can observe that the value of this frequency is slightly shifted due to the fact that in **3b** there is less contacts with neighboring ring structures. In most of the other structures this shift is relatively consistant and shows small displacements from the mean behavior. The peaks that we calculated for **3b** are at 1516 cm^{-1} which are in excellent agreement to those experimentally verified. The others at 2990 cm^{-1} are found at around 3010 in the 3b species and slightly higher for the others. The peaks that were found at 2359 cm^{-1} experimentally are not found on the theoretical spectra and this may be accounted for due to impurities. For the most part it is safe to assume that the experimental and theoretical separations in the observed vibrational spectra are in fact minimal and do conincide on many observed fundamental bands.

Also, in **3a**, **3c, 3e** we observe peaks at 1550, 1585 and at 1534 cm^{-1}, respectively. Perhaps these may añsp be characterized as C=O stretches but the values vary based on the environment and torsional angles that separate the structural features of each. We can also see that a very high band at around 1750 cm^{-1} in all structures that may consistute non-fundamental modes. In the 1562 cm^{-1} there are also N-H modes, which are presented at 1560, 1565, 1573, 1578, 1580, 1601 cm^{-1} for **3a-3f** respectively, that should also contribute. Perhaps these may also be a mixture of δ_{as} $(CH_3)/(CH_2)$ scissoring modes, since they tend to occur in the same region[16].

While we have only considered fundamental modes there is some knowledge available on the overtones and hot transitions for certain species[14] from a theoretical perspective. Experimentally, there is very little knowledge known about the hot transitions and overtones in molecules of this type. However, other investigations have shown that hot transitions and overtones can be adequately accounted for (in correlation to experiments) by using DFT methods and gaussian basis sets[15]. To the best of our knowledge limited information on these data points are available for the compounds investigated herein. The B3LYP/6-31G* basis set has been shown to adequately reproduce vibrational frequencies for large scale systems to a reasonably good level of approximation[9,17-19]. We attempted a test calculation at the B3LYP/6-311++G** level of theory and as a result the differences in energies and vibrational frequencies for the **3b**/**3f** separation are minimal. The results computed with the current basis yield decent geometries and structures which posses a high level of precision. Additionally, since these systems are large it is difficult to conduct such a calculation in a timely fashion.

As for the NMR frequencies limited information with regards to the experimental data can be made. The only useful conclusion that can be made is that the ^{13}C band correspond to a shift at 196.3, 136.1 is compared to the theoretical values of 197.2, 142.1 computed at the DFT level for **3b**. For **3f** these values are around 200.1 and 143.2 ppm which can be attributed to the addition of electron withdrawing NH groups that arise from the tautomerization process. The NH shift observed for the ^{1}H shift is experimentally measured at around 12.48 compared to 13.51 ppm computed for **3b** at the DFT level of theory. For **3f** we computed the same shift to be 11.45 which again has to do with steric hindrance and the electronic configuration surrounding the group in this configuration. For the other structures these shifts are quite different and probably will not be located experimentally.

Tables 1-2 shows the thermodynamic parameters for the product (**3**) where T (temperature in K), S (entropy in J mol^{-1} K^{-1}), C_p (heat capacity at constant pressure in kJ mol^{-1} K^{-1}), and $\Delta H = H° - H°_{298.15}$ (enthalpy content, in kJ mol^{-1}), T_1 = 100 K, T_2=298.15 K, and T_3 = 1000 K calculated using the B3LYP/6-31G* frequencies. These calculations are useful for future thermodynamic studies as well as for NIST database indexing. As we can see the structures (generally) with the highest values have the most stability. Therefore, **3a**, **3f,** are the highest, **3b**, **3d** are next, and **3e**, **3c** are last in agreement with the theoretical data in Table 2.

Table 2. Physical properties of the computed at the B3LYP/6-31G* level of theory

		Fitted Thermodynamic Equation (T/1000=t)	100 K	298.15 K	1000 K
A	C_p	-10.95834+1364.69249*t -766.8094*t^2 +146.09866*t^3 +0.40541*t^{-2}	158.25	334.11	734.36
	S	-26.75076*ln(t) +1422.85162*t -830.53165*t^2/2 +164.74934*t^3/3 -0.66038/(2*t^2) +256.28201	423.05	673.81	1318.51
	ΔH	-44.86196*t + 1513.37057*t^2/2 -979.67276*t^3/3 +243.47281*t^4/4 -0.83964/t +15.98145	10.35	58.93	461.29
B	C_p	-7.20047+ 1378.74054*t -808.96602*t^2 +170.04975*t^3 +0.31466*t^{-2}	153.98	338.23	733.73
	S	-20.17836*ln(t) +1426.05659*t -859.77852*t^2/2 +184.19795*t^3/3 -0.52599/(2*t^2) +241.56582	400.10	651.71	1298.92
	ΔH	-36.26937*t + 1506.58649*t^2/2 +-992.66411*t^3/3 +254.45901*t^4/4 +-0.68458/t +12.80987	9.55	58.44	461.89
C	C_p	-3.37434+ 1377.99661*t -808.16988*t^2 +167.8286*t^3 +0.27362*t^{-2}	153.61	341.20	735.42
	S	-17.75474*ln(t) +1430.98747*t -865.92931*t^2/2 +184.40175*t^3/3 -0.50368/(2*t^2) +246.45792	400.99	655.00	1298.92
	ΔH	-35.23684*t + 1518.15965*t^2/2 -1009.42832*t^3/3 +260.18884*t^4/4 -0.67704/t +12.47863	9.45	58.82	461.89
D	C_p	-0.10354+1274.20808*t -678.42267*t^2 +113.63308*t^3 +0.30995*t^{-2}	151.35	323.85	710.63
	S	-14.6428*ln(t) +1324.98563*t -728.08641*t^2/2 +123.91453*t^3/3 -0.55496/(2*t^2) +275.47841	410.35	653.97	1277.51
	ΔH	-34.77286*t + 1425.66071*t^2/2 -894.15979*t^3/3 +211.72395*t^4/4 -0.75245/t +13.82095	9.66	56.87	446.02
E	C_p	-7.6486+ 1372.71648*t -789.17445*t^2 157.71952 *t^3 +0.33431*t^{-2}	155.05	337.41	734.84
	S	-22.2462*ln(t) +1425.99658*t -846.37765*t^2/2 +173.58239*t^3/3 -0.5713/(2*t^2) +249.83184	410.92	662.72	1310.27
	ΔH	-39.76673*t + 1513.52238*t^2/2 -990.64763*t^3/3 +249.81791*t^4/4 +-0.74378/t +14.00609	9.84	58.72	462.51
F	C_p	-15.88241+ 1379.03784*t -784.06624*t^2 +153.12351*t^3 + 0.40863*t^{-2}	154.92	332.18	733.54
	S	-31.96804*ln(t) + 1438.71825*t -850.38098*t^2/2 + 173.18847*t^3/3 -0.66643/(2*t^2) + 247.7713	427.74	675.5	1318.75
	ΔH	-50.72143*t +1532.26233*t^2/2 -1004.37219*t^3/3 + 254.46641*t^4/4 -0.85273/t + 16.47185	10.21	58.27	459.87

Crystal structure analysis

The crystal structure of **3b**, $C_{16}H_{20}N_2O_2$, has been determined at room temperature. Molecules crystallize in the orthorhombic space group ***Pbcn*** and the asymmetric unit contains only one half-molecule. The molecule lies on a twofold rotation axis and hence posses C2 molecular symmetry.

The crystallographic details have been provided in Table 3 and the structure was solved by direct methods and refined by least-squares on F_{obs}^2 by using the SIR-97 and SHELXL-97 programs, respectively.[10,11] All H atoms were geometrically located to the ideal positions and treated as riding atoms, with N—H = 0.86, C—H = 0.93 - 0.96 Å and $U_{iso}(H) = 1.5U_{eq}(C)$ for methyl H atoms or $U_{iso}(H) = 1.2U_{eq}(C)$ for the other H atoms.

Table 3. Crystal, X-ray data collection and refinement parameters for **3b**

Formula	$C_{16}H_{20}N_2O_2$
Molecular weight (g mol^{-1})	272.34
Crystal system	Orthorhombic
Space group	*Pbcn*
Z	4
Temperature (K)	296(2)
F (000)	584
Crystal size (mm)	0.64 × 0.52 × 0.43 mm
a (Å)	10.8412 (10)
b (Å)	8.9205 (7)
c (Å)	14.9949 (13)
V (Å^3)	1450.1 (2)
μ (MoKα_1) (mm^{-1})	0.08
Calculated density (g cm^{-3})	1.247
θ range	2.96–27.93
Number of reflections	6824
No. of unique reflections	1687
No. of reflections obsd ($I > 2\sigma(I)$)	1330
Parameters refined	94
R ($I > 2\sigma(I)$)	0.038
R_w	0.111
Goodness of fit	1.05
Diff. Fourier residues (e$^-$ Å^{-3}) Max/Min	0.17 /−0.16

The molecule, **3b**, is shown in Figure 3; the final atomic coordinates and equivalent isotropic thermal parameters for non-hydrogen atoms are listed in Table 3, with selected bond angles and hydrogen-bond parameters in Tables 4 and 5, respectively. In the crystal structure of **3b**, the asymmetric unit contains only one half-molecule. A twofold rotation axis passes midline through

the phenyl ring atoms at the C7, C6 and C8 positions for which the bond lengths and angles are within normal ranges.[12] The central ring A (C6 - C8 / C7a / C6a / C8a) is, of course, planar and the O1/N1/C1–C5 group is nearly planar, with a puckering amplitude of QT = 0.1026 (2) Å[13] with the dihedral angles between these planes being 46.6(2)°. The crystal packing is along the a axis which is depicted in Figure 5.

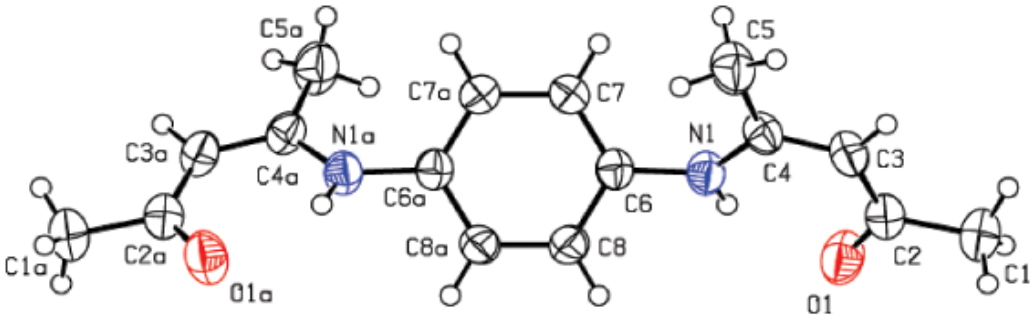

Figure 3. The molecular structure of the title compound, showing the atom labeling scheme. Ellipsoids represent displacement parameters at the 50% probability level [Symmetry codes: (a) −x, y, 1/2 − z].

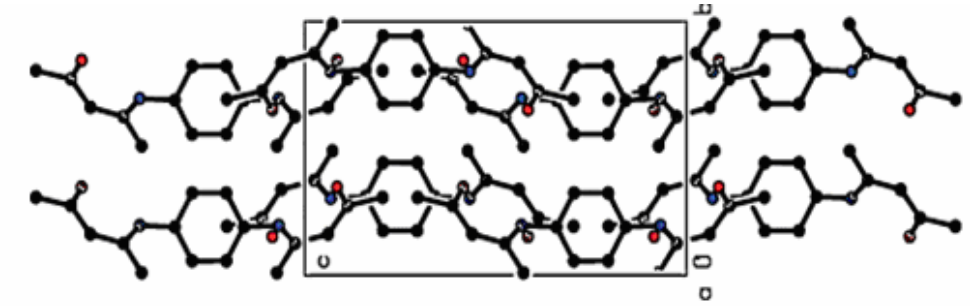

Figure 4. The crystal packing of **3b**, viewed along the **a** axis.

Table 4. Selected geometric parameters (Å, °) for **3b**, with the B3LYP/6-31G* values shown in parenthesis []

C1—C2	1.5058 (17) [1.5075]	C6—C7	1.3849 (16) [1.3805]
C2—O1	1.2428 (15) [1.2301]	C6—C8	1.3895 (15) [1.3892]
C2—C3	1.4147 (18) [1.3905]	C6—N1	1.4156 (14) [1.4204]
C3—C4	1.3744 (16) [1.3600]	C7—C7^{i}	1.386 (2) [1.3861]
C4—N1	1.3488 (14)	C8—C8^{i}	1.384 (2)

	[1.3900]		[1.3850]
C4—C5	1.4949 (17)		
	[1.4802]		
O1—C2—C3	123.38 (11)	C7—C6—C8	118.83 (11)
	[126.501]		[120.20]
O1—C2—C1	118.77 (12)	C7—C6—N1	122.91 (10)
	[111.40]		[121.32]
C3—C2—C1	117.84 (11)	C8—C6—N1	118.24 (10)
	[113.10]		[118.10]
C4—C3—C2	124.91 (11)	C6—C7—C7^{i}	120.59 (6)
	[126.20]		[120.30]
N1—C4—C3	120.51 (11)	C8^{i}—C8—C6	120.55 (7)
	[121.30]		[120.61]
N1—C4—C5	119.94 (10)	C4—N1—C6	128.04 (10)
	[118.60]		[119.01]

Symmetry codes: (i) −x, y, 1/2 − z.

Table 5. Hydrogen-bond geometry (Å, °) for **3b**

D—H···*A*	*D*—H	H···*A*	*D*···*A*	*D*—H···*A*
N1—H1···O1	0.86	2.00	2.6717 (15)	134

Supplementary information

Crystallographic data for the structural analysis have been deposited with the Cambridge crystallographic Data Centre, CCDC 642007 for compound **3**. Copies of this information can be obtained free of charge from The Director, CCDC, 12 Union Road, Cambridge, CB2 1EZ, UK (fax: +44-1223-336033; e-mail: deposit@ccdc.cam.ac.uk or http://www.ccdc.cam.ac.uk).

Conclusions

We have decided to compare the AM1 and DFT methods since they are both semi-empirically derived methods[9] and a comparison can be instructive for workers in the field. It is important to note that the flexibility in the hydrocarbon backbone may lead to experimental difficulties in locating the lowest energy structures. Both theoretical methods propose that **3f** is the lowest in energy but experimentally **3b** is observed. It is our belief that **3f** should be found experimentally but further laboratory investigations must be pursued to solidify this claim. Perhaps the symmetrical nature of the **3b** system leads to its abundance in nature, but other routes towards

the asymmetrical synthesis of **3f** should be feasible which is currently under active investigation in our collaborative teams.

The computed geometrical parameters adequately demonstrate that the two structures share a physical resemblance to the experimental data. Even more interesting is the correlation between the AM1 and B3LYP levels of theory that suggests that low level calculations qualitatively are in agreement to the correlated DFT methods. Energetic analysis shows that the lowest isomer is the **3f** species which is physically realistic due to the limitations on the steric effects. Further experimental elucidation is necessary before such claim can be adequately demonstrated.

Experimental Section

General Procedures. NMR spectra (^{1}H, ^{13}C) were recorded on a Bruker AM 300 (operating at 300.13 MHz for ^{1}H, at 75.47 MHz for ^{13}C) spectrometer. NMR data are listed in ppm and are reported relative to tetra-methylsilane (^{1}H, ^{13}C), residual solvent peaks being used as internal standard. Complete assignments of the ^{13}C spectra required non-decoupled ^{13}C NMR spectra with selective ^{1}H decoupling. Infrared spectra were recorded in KBr pellets using a Brucker IFS28 FTIR spectrometer.

Synthetic Methodology

To a stirred solution of o-phenylenediamine (**1**; 4 g, 37 mmol) in ethanol (70 mL), the 2,4-pentanedione or acetylacetone (**2**; 7.6 g, 76 mmol) in 70 ml of absolute ethanol, was added drop wise via syringe at room temperature during ca 10 min. After an additional 10 min of stirring, the mixture was stirred and heated in a refluxing ethanol solution for 24 h. At which point the solvent was eliminated using a rota-evaporator apparatus. The precipitate was filtered, washed with water (3×15 mL), and then dissolved in CH_2Cl_2 (40 mL). After drying with anhydrous $MgSO_4$ and evaporation of the solvent, the residue was recrystallised: CH_2Cl_2 / ether, 1: 1) to give pure white crystals of product **3** (67% yield). Mp = 178-180 °C. R_f = 0.35 (Hexane/ diethylether): (1/2). IR (KBr) υ cm^{-1}: 2990; 2359; 1562 (C=O); 1514 (C=N). ^{1}H NMR (300 MHz, $CDCl_3$) δ ppm: 12.48 (s, 2H, N<u>H</u>); 7.07 (s, 4H, Ph); 5.20 (s, 2H, 2C<u>H</u>=C); 2.1 (s, 6H, 2C<u>H</u>$_3$C=O); 2.0 (s, 6H, 2C<u>H</u>$_3$ C-N= C). ^{13}C NMR (75.47 MHz, $CDCl_3$) δppm: 196.27; 159.84; 136.09; 125.12; 97.91; 29.19; 19.84. SM (IC, CH_4): m/z: $[M+H]^{+\cdot}$ = 273; $[M]^{+\cdot}$ = 272; 282; 257; 229; 215; 190; 174; 160.

Acknowledgements

We are indebted to the "Project Global de la Recherche à l'Université Mohammed Premier PGR-UMP-BH-2005" and the CUD-UMP-BH-2007 for financial support.

References

1. (a) Le Bozec, H.; Le Bouder, T.; Maury, O.; Ledoux, I.; Zyss, J. *Journal of Optics A: Pure and Applied Optics* **2002**, *4*, S189. (b) Maury, O.; Guégan, J.-P.; Renouard, T.; Hilton, A.; Dupau, P.; Sandon, N.; Toupet, L.; Le Bozec H. *New J. Chem.* **2001**, *25*, 1553.
2. (a) Bourgault, M.; Baum, K.; Le Bozec, H.; Ledoux, I.; Pucetti, G.; Zyss, J. *New. J. Chem*. **1998,** 512. (b) Renouard, T.; Le Bozec, H.; Ledoux, I.; Zyss, J. *Chem. Commun*. **1999**, 871. (c) Renouard, T.; Le Bozec, H. *Eur. J. Inorg. Chem*. (Review), **2000**, 229.
3. Hilton, A.; Renouard, T.; Maury, O.; Le Bozec, H.; Ledoux, I. Zyss, J. *Chem. Commun*. **1999**, 2521.
4. Viau, L.; Sénéchal, K.; Maury, O.; Guégan, J-P.; Dupau, P.; Toupet, L.; Le Bozec, H. *Synthesis* **2003**, 577.
5. (a) McCarthy, P. J.; Hovey, R. J.; Ueno, K.; Martell, A. E. *J. Am. Chem. Soc*., **1955**, *77*, 5820. (b) Hovey, R. J.; O'Connell, J. J.; Martell, A. E. *J. Am. Chem. Soc.* **1959***, 81*, 3189. (c) Dey, K.; Maiti, R. K.; Bhar, J. K. *Transition Met. Chem*. **1981**, *6*, 346. (d) Nathan, L. C.; Traina, C. A. *Polyhedron* **2003**, *22*, 3213.
6. (a) Hakkou, A.; Bouakka, M.; Touzani, R.; Elkadiri, S.; Ramdani, A.; Kotchevar, A.; Ellis, T.; Waring, M.; Ben Hadda T. *Molecules* **2002**, *7*, 641. (b) Anaflous, A.; Benchat, N.; Mimouni, M.; Abouricha, S.; Ben Hadda, T.; El-Bali, B.; Hakkou A.; Hacht B. *Letters in Drug Design &Discovery*, **2004**, *1*, 224. (c) Aggarwal, R. C.; Narayana, D. S., *Ind. J. Chem. Sect.A: Inorg., Phys., Theor. Analy*. **1984**, *23A*, 920.
7. Frisch, M. J.; Trucks, G. W.; Schlegel, H. B.; Scuseria, G. E.; Robb, M. A.; Cheeseman, J. R.; Montgomery, J. A.; Vreven, Jr., T.; Kudin, K. N.; Burant, J. C.; Millam, J. M.; Iyengar, S. S.; Tomasi, J.; Barone, V.; Mennucci, B.; Cossi, M.; Scalmani, G.; Rega, N.; Petersson, G. A.; Nakatsuji, H.; Hada, M.; Ehara, M.; Toyota, K.; Fukuda, R.; Hasegawa, J.; Ishida, M.; Nakajima, T.; Honda, Y.; Kitao, O.; Nakai, H.; Klene, M.; Li, X.; Knox, J. E.; Hratchian, H. P.; Cross, J. B.; Adamo, C.; Jaramillo, J.; Gomperts, R.; Stratmann, R. E.; Yazyev, O.; Austin, A. J.; Cammi, R.; Pomelli, C.; Ochterski, J. W.; Ayala, P. Y.; Morokuma, K.; Voth, G. A.; Salvador, P.; Dannenberg, J. J.; Zakrzewski, V. G.; Dapprich, S.; Daniels, A. D.; Strain, M. C.; Farkas, O.; Malick, D. K.; Rabuck, A. D.; Raghavachari, K.; Foresman, J. B.; Ortiz, J. V.; Cui, Q.; Baboul, A. G.; Clifford, S.; Cioslowski, J.; Stefanov, B. B.; Liu, G.; Liashenko, A;. Piskorz, P.; Komaromi, I.; Martin, R. L.; Fox, D. J.; Keith, T.; Al-Laham, M. A.; Peng, C. Y.; Nanayakkara, A.; Challacombe, M.; Gill, P. M. W.; Johnson, B.; Chen, W.; Wong, M. W.; Gonzalez, C.; Pople, J. A. Gaussian, Inc., GAUSSIAN03, Revision B.05，Pittsburgh PA, 2003.
8. Foresman, J. B.; Frisch, A. E. *Exploring Chemistry with Electronic Structure Methods*, 2nd edition Gaussian, Inc.: Pittsburgh, 1996.
9. Jalbout, A. F.; Nazari, F.; Turker L. *J. Mol. Struct. (THEOCHEM)*, **2004**, *1*, 627.
10. Altomare, A.; Burla, M. C.; Camalli, M.; Cascarano, G. L.; Giacovazzo, C.; Guagliardi, A.; Moliterni, A. G.;. Polidori and, G.; Spagna, R., *J. Appl. Cryst.* **1999**, *32*, 115.

11. Sheldrick, G. M., 1997, SHELXL97: University of Goettingen, Germany.
12. Allen, F. H.; Kennard, O.; Watson, D. G.; Brammer, L.; Orpen, A. G.; Taylor R. *J. Chem. Soc., Perkin Trans*. **1987**, *2*, S1.
13. Cremer, D.; Pople, J. A. *J. Am. Chem. Soc*. **1975**, *97*, 1354.
14. Schmatz, S. *J. Chem. Phys*. **2005**, *122*, 234306/1.
15. Balazic, K.; Stare, J.; Mavri, J. *J. Chem. Inf. Mod*. **2007**, *47*, 832.
16. Jalbout, A. F.; Ouasri, A.; Jeghnou, H.; Rhandour, A. *Vibrat. Spect*. **2007**, *44*, 94.
17. (a) Jalbout, A. F.; Hameed, A. J.; Trzaskowski, B. *J. Organomet. Chem*. **2007***, 692*, 1039. (b) Jalbout, A. F., Trzaskowski, B., Hameed, A. J. *J. Organomet. Chem*. **2006***, 691*, 4589.
18. Bennani, B.; Jalbout, A. F.; Baba, B. F.; Larbi, N. B.; Boukir, A.; Kerbal, A.; Mimouni, M.; Hadda, T. B.; Trzaskowski, B. *J. Heterocycl. Chem.* **2007**, *44*, 711.
19. Jalbout, A. F.; Li, X.-H.; Trzaskowski, B.; Raissi, H. *Eclet. Quim.* **2006**, *31*, 53.